Environmental Modelling and Software 107 (2018) 307–320

Contents lists available at ScienceDirect

Environmental Modelling & Software

journal homepage: www.elsevier.com/locate/envsoft

An improved nightlight-based method for modeling urban CO_2 emissions

Ji Han[a,h,*], Xing Meng[b], Hanwei Liang[c], Zhi Cao[d,e], Liang Dong[f,g], Cheng Huang[b]

[a] Shanghai Key Laboratory for Urban Ecological Processes and Eco-Restoration, School of Ecological and Environmental Sciences, East China Normal University, Shanghai 200041, China
[b] School of Geographical Sciences, East China Normal University, Shanghai 200041, China
[c] Collaborative Innovation Center on Forecast and Evaluation of Meteorological Disaster, Nanjing University of Information Science & Technology, Nanjing 210044, China
[d] Institute of Geographic Sciences and Nature Resources Research, Chinese Academy of Sciences, 11A Datun Road, Beijing 100101, China
[e] SDU Life Cycle Engineering, Department of Chemical Engineering, Biotechnology and Environmental Technology, University of Southern Denmark, Campusvej 55, 5230 Odense M, Denmark
[f] Institute of Environmental Sciences, CML, Leiden University, Einsteinweg 2, 2333 CC Leiden, the Netherlands
[g] Center for Social and Environmental System Research, National Institute for Environmental Studies, 16-2 Onogawa, Tsukuba-City, Ibaraki 305-8506, Japan
[h] Institute of Eco-Chongming (IEC), 3663 N. Zhongshan Rd., Shanghai 200062, Japan

ARTICLE INFO

Keywords:
Urban CO_2 emissions
Nighttime light
Panel-data regression
Yangtze river delta

ABSTRACT

An accurate modeling of urban CO_2 emissions is important for understanding the dynamics of carbon cycle and for designing low-carbon policies. We develop an improved nightlight-based method to model urban CO_2 emissions and investigate their spatiotemporal patterns. Differing from the previous methods, in processing the pre-modeling data, we bring forward the existing CO_2 inventories from national and provincial levels to city level, and correct the saturation and blooming problems of nightlight. In modeling the correlation between nightlight and statistically accounted CO_2 emissions, we highlight a panel-data regression analysis that considers the spatiotemporal heterogeneity across cities and over time simultaneously. Eleven cities in Yangtze River Delta of China were selected for a case study testing our method. The internal and external validations have proven the predominance of our proposed method for capturing the nightlight-CO_2 correlation, and for describing the spatial distribution and heterogeneity of urban CO_2 emissions.

1. Introduction

Cities are the main contributor to climate change, since they are responsible for more than 70% of the global fossil-fuel-induced carbon emissions, while occupying less than 2% of the earth's land area (Gurney et al., 2015). Their impacts are expected to grow due to continuous urbanization. China has been urbanizing at an unprecedented speed and has become the largest carbon emitter in the world. The proportion of residences qualifying as urban increased from 18% in 1978 to 55% in 2013. The number of prefecture-level cities with population sizes over one million also expanded to 133 (NBS, 2015). Consequently, some Chinese mega cities, such as Shanghai, emitted more greenhouse gases than several countries did, such as Thailand and the Netherlands (World Bank, 2010). Therefore, the reduction in carbon emissions at a city scale becomes increasingly important and urgent.

A long-term monitoring of urban CO_2 emissions is critical for understanding the dynamic patterns and drivers of the carbon cycle and for helping policymakers to design effective policies to mitigate climate change. Based on Intergovernmental Panel on Climate Change (IPCC) guidelines for national greenhouse gas accounting, a growing number of scholars and research institutes have developed methodologies and tools for quantifying carbon emissions at a city scale, including the International Local Government Greenhouse Gas Emission Analysis Protocol (ICLEI, 2009), the GHG Protocol (WBCSD and WRI, 2004), the Greenhouse Gas Regional Inventory Protocol (Carney et al., 2009), and the Sustainable Energy Action Plan (SEAP) (CoM, 2010). However, despite recent advancements in research aimed at estimating the dynamics of urban carbon emissions, great challenges remain that are largely due to the lack of comprehensive, consistent and comparable statistical data on energy consumption and human activities on a city scale. Furthermore, all of the accounting methods based on energy statistics all treat the city as a homogenous unit but represent the dynamics of the urbanization processes, such as the rapid sprawl of urban built-up areas, poorly (Albert et al., 2015; Edward and Matthew, 2010).

As means of addressing the abovementioned challenges, nighttime light (NTL) has been widely used as a useful proxy for economic output

* Corresponding author. Shanghai Key Laboratory for Urban Ecological Processes and Eco-Restoration, School of Ecological and Environmental Sciences, East China Normal University, Shanghai 200041, China.
E-mail address: jhan@re.ecnu.edu.cn (J. Han).

https://doi.org/10.1016/j.envsoft.2018.05.008
Received 29 November 2017; Received in revised form 23 February 2018; Accepted 21 May 2018
Available online 22 June 2018
1364-8152/

(Chen and Nordhaus, 2011), urban extent extraction (Xie and Weng, 2017), population estimation (Sutton et al., 2001), electricity consumption (Cao et al., 2014), and in-use metal stocks (Liang et al., 2014) due to its strong correlation with human activities and its availability at a high spatial resolution for most of the world, beginning in 1992. Recently, this proxy has also been applied to estimate urban CO_2 emissions at different time and space scales. For example, Oda and Maksyutov (2011) downscaled national CO_2 emissions to global 1 km × 1 km grids using nightlight as a proxy and separately allocated the point source emissions based on the global power plant database. Asefi-Najafabady et al. (2014) built upon a previously developed fossil fuel data assimilation system (FFDAS) and expanded the estimated 1 km gridded CO_2 emissions from a single year to multi-years from 1997 to 2010 by combining with nightlight data, gridded population, and global power plant database. Su et al. (2014) analyzed the linear correlation between CO_2 emissions and NTL in provinces and a limited number of cities of China based on a pool-data regression analysis without considering the differences across regions and over time, and predicted the carbon emissions in cities without direct energy data. Meng et al. (2014) and Shi et al. (2016) developed a panel-data regression model that took into account the city-specific coefficient in capturing the relationships between province-level energy-related CO_2 emissions in China with NTL and downscaled the emissions to an urban or 1 km scale. These studies have reached a consensus that the NTL can be used as a valid and useful proxy for downscaling statistically accounted CO_2 emissions to scale of interest (for example, pixel, urban, city, and urban agglomeration). And one can obtain estimates that are much more geographically consistent than energy consumption statistics through bypassing the reliance on statistical energy consumption data.

However, at least three aspects can be substantially improved. First, a suitable carbon accounting method needs to be selected that is compatible with the available energy statistics. The IPCC guidelines are based on detailed energy consumption data by sector and fuel type and are the most preferred and commonly used approach in the existing literature (Oda and Maksyutov, 2011; Meng et al., 2014; Su et al., 2014; Shi et al., 2016). However, detailed energy data are not always available for cities. Taking China as an example, the energy balance table is only available for the whole country, provinces and a limited number of cities, such as Shanghai, Guangzhou, and Shenzhen. In most cities, only certain fragmented information about energy consumption in certain specific sectors (e.g., industrial enterprises and households) can be accessed through the city's statistical yearbook. Thus, the scope and methodological complexity should be taken into account in choosing an appropriate accounting method so a more exact correlation between carbon emissions and NTL can be derived. Second, the intrinsic saturation problem of NTL especially in the city centers needs to be addressed; otherwise it may constrain NTL's further application and estimation accuracy. Internationally, there are a great number of studies focusing on saturation correction. Various methods and indices have been developed generally by combining original NTL with other data sources (such as Normalized Difference Vegetation Index (NDVI), and population density) to increase the variation of NTL in urban cores (Meng et al., 2014; Ma et al., 2017). However, potential improvements still exist in relieving the saturation issue (Bennett and Smith, 2017). Third, the spatiotemporal heterogeneity across cities and over time must be considered. The socioeconomic and geographical conditions usually vary in different cities and at different development stages, even for the same city. These differences may result in significant disparities in both the quantity and change patterns of carbon emissions.

This study aims to address the abovementioned deficiencies so as to better estimate urban CO_2 emissions. In processing the pre-modeling data, we bring forward the existing CO_2 inventories from national and provincial levels to city level, which to some extent breaks through the strong requirement on detailed statistical energy data, and raise the accuracy of pixel-level CO_2 estimation as it is downscaled from city level rather than from country and province. Moreover, we correct the saturation and blooming problems of NTL by integrating time-series NDVI and population density data, which reduces the estimation error in the urban core and rural areas. In modeling the correlation between NTL and statistically accounted CO_2 emissions, we propose a panel-data regression model, which considers the spatiotemporal heterogeneities across cities and over time simultaneously. Eleven cities in the Yangtze River Delta (YRD) of China were selected as a case to test the method. Based on the same dataset, our model was internally validated through a 2-fold cross-validation process and compared with a pool-data regression model and a panel-data regression model that only considers city-specific coefficient. In addition, our model was also externally validated with other studies both at city and pixel level. By doing so, the predominance of our improved method could be seen clearly. Finally, the uncertainties, limitations and potential improvements have also been discussed.

2. Study area and data

2.1. Study area

YRD is China's largest urban cluster, wherein 11 cities were selected for case studies (Fig. 1). There are three reasons for their selection. The first is the important role that the YRD plays in socioeconomic development and carbon emissions. It is one of the most rapidly urbanizing and wealthiest regions in China, with the country's largest urban cluster, covering 2% of the country's territory but contributing 20% and 12% to the total GDP and CO_2 emissions, respectively, in 2005 (Cai and Xie, 2007). The second reason is the relatively lower disparity in societal and natural conditions (e.g., culture, lifestyle, income level and climate) among the cities in the YRD compared to broader areas across China. Choosing a study area with less regional disparity may reduce the disturbance from spatial heterogeneity in correlation analyses between carbon and NTL. The third reason was that the 11 case study cities reflect some generalities of economic structure and transport development of Chinese cities. As shown in Table S1 in the Supplementary Material, some cities in the YRD (for example, Huzhou and Suzhou) have developed the secondary industry as their leading industry, which is consistent with most cities in middle reaches of the Yellow River, the middle reaches of the Yangtze River, and in the northeastern regions. However, there are also cities in the YRD (for example, Shanghai and Hangzhou) whose tertiary industry is the pillar industry. It represents a widely existing situation in the eastern coastal and northern coastal cities in China. For the transport sector, there is a common phenomenon not only in the YRD cities but also across China that the number of civil automobiles has been increasing sharply at a mean annual rate of more than 13% between 2003 and 2013 (NBS, 2015). In summary, owing to the important role, lower disparity and representative generality, we believe that the YRD is a good case study area for both testing our proposed method and increasing our understanding of urban CO_2 emissions in China.

2.2. Description of the data

Table 1 outlines the data used for the analysis, which generally includes two kinds, with a time range from 2003 to 2013. One is the spatial data including NTL produced by the Defense Meteorological Satellite Program's Operational Linescan System (DMSP-OLS), land use and land cover data classified based on Landsat Enhanced Thematic Mapper Plus (Landsat ETM+) images, NDVI data based on Moderate-resolution Imaging Spectroradiomet (MODIS) from United State Geographic Survey (http://www.usgs.gov), and population density data. The nighttime light data (version 4) have a spatial resolution of 1 km × 1 km, and its digital number (DN) values of the artificial nighttime light brightness from cities, towns, and other sites ranged from 0 to 63. These data can be accessed online from the National

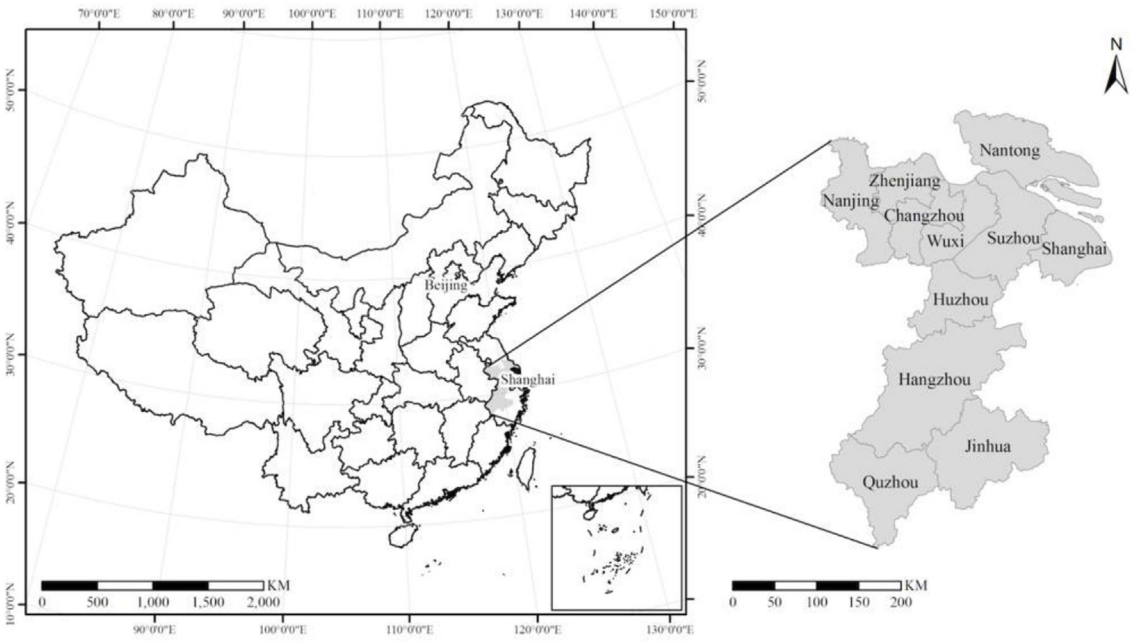

Fig. 1. Location of the case study cities in the YRD, China.

Geophysical Data Center at NOAA, USA (http://ngdc.noaa.gov/eog/). The monthly composite NDVI in China after splicing, cutting and re-projection was download from the Resources and Environmental Sciences International Scientific & Technical Data Mirror Site, Computer Network Information Center (http://www.gscloud.cn). The land use data including 6 land types (urban built-up, cropland, water, forest, grassland, others) as well as the population density data were obtained from the Data Center for Resources and Environmental Sciences, Chinese Academy of Sciences (http://www.resdc.cn). The other data include the city-level statistics for CO_2 accounting. The direct energy consumption data by industry, commercial and household sectors, together with the vehicle fleet number of all eleven cities, were compiled from the statistical yearbooks of each city, Jiangsu and Zhejiang provinces, and China overall.

3. Methodology

Generally, the method that uses NTL to downscale statistically accounted CO_2 emissions to scale of interest (for example, pixel, urban, and etc.) is based on a hypothesis that the pixel-level NTL's brightness has a positive correlation with the energy consumption related CO_2 emissions from the same pixel. In our study, in order to downscale city-level accounted CO_2 emissions to urban scale, there are basically two major steps. The first is to process the pre-modeling data, which contains the city-level CO_2 accounting, and NTL data correction and urban extent extraction. The second is to model urban CO_2 emissions through building the correlation between accounted emission and NTL, and estimating pixel-level emissions and aggregating them to urban scale.

3.1. Pre-modeling data processing

3.1.1. City-level CO_2 accounting and uncertainty quantification

As defined in the corporate accounting and reporting standards, which were developed by the World Resources Institute and the World Business Council for Sustainable Development (WRI/WBCSD) and are widely used by researchers, the city-level carbon inventories generally

Table 1
Data used in this study.

Data type	Content		Space & time resolution	Source
Remote sensing and GIS data	DMSP-OLS nighttime light (Version 4)		1 km × 1 km 2003–2013	National Geophysical Data Center of NOAA (http://ngdc.noaa.gov/eog/)
	MODIS monthly composite NDVI		500 m × 500 m 2003–2013	United State Geographic Survey (http://www.usgs.gov); International Scientific & Technical Data Mirror Site, Computer Network Information Center (http://www.gscloud.cn)
	Population density		1 km × 1 km 2000, 2005, 2010	Resources and Environmental Sciences Data Center (http://www.resdc.cn)
	Land use and cover data classified from Landsat ETM + images		30 m × 30 m 2000, 2005, 2010	United State Geographic Survey (http://www.usgs.gov); Data Center for Resources and Environmental Sciences, Chinese Academy of Sciences (http://www.resdc.cn.)
Statistical data	Industrial sector	Fossil fuel consumption, such as coal, oil, natural gas, and electricity	City level 2003–2013	Statistical yearbooks of each city; Statistical Yearbook of Jiangsu Province; Statistical Yearbook of Zhejiang Province; China Statistical Yearbook
	Commercial sector	Electricity consumption		
	Household sector	Consumption of natural gas, liquefied natural gas, liquefied petroleum gas, coal gas, and electricity		
	Transport sector	Fleet number, such as bus, taxi, passenger vehicle, truck, motorcycle		

include three scopes of operational boundaries (WBCSD and WRI, 2004). Scope 1 is the direct emissions from activities that occurred within the physical boundary of a city, such as emissions from factories, vehicles, and households. Scope 2 incorporates the emissions outside of a city but is related to energy use within a city, which includes the electricity and heat produced elsewhere. Scope 3 is more comprehensive than scopes 1 and 2; it considers both the direct and embodied emissions during life-cycle processes of products and services consumed in the city. Scope 3 includes the emissions from waste disposal, air transport, those embodied in food, water, and construction materials, and others. Usually, the basic carbon inventory for most cities refers to scope 1 and 2 emissions (for example, Kennedy et al., 2010; Yu et al., 2012). However, those including Scope 3 emissions are mostly reported in urban metabolism studies (for example, Kennedy et al., 2009). Obviously, the more scopes included in inventory accounting, the more it requires extensive data, processing time and expertise (Whittaker et al., 2013). Due to the features of appropriate coverage of carbon emission scopes and moderate difficulty in accounting, the SEAP approach (Yamina et al., 2014) is employed in this study since it fits within scope 1 and 2 emissions, in which city-level CO_2 emissions include direct emissions generated inside of a city boundary, such as the combustion of coal and oil in industrial enterprises, and the indirect emissions from electricity consumption and heating that are mainly produced outside of cities. In the accounting, the SEAP method estimates the CO_2 emissions from stationary and mobile sources in a city (Fig. 2). The stationary emissions include those from energy consumption in industrial, tertiary and household sectors, whereas the mobile emissions are derived from public, private and commercial transport sectors.

Specifically, the accounted stationary emissions ($AE_{stationary}$) are estimated by Eq. (1).

$$AE_{stationary} = \sum_{m,n,t} (EC_{m,n,t} \times NCV_{m,n} \times EF_{m,n}) \quad (1)$$

where, *m, n* and *t* represent the investigated sector, fuel type and year respectively; EC represents the amount of energy consumption (in metric tons); NCV represents the net calorific value (in megawatts per ton, MWh/t); EF represents the CO_2 emission factor (in tons CO_2 per megawatts, tCO_2/MWh). The details can be found in Table 2.

The accounted mobile emissions (AE_{mobile}) are estimated by Eq. (2).

$$AE_{mobile} = \sum_{v,n,t} \left(FN_{v,n,t} \times VKT_{v,n,t} \times FE_{v,n,t} \times D_n \times CR_n \times \frac{44}{12} \right) \quad (2)$$

where, *v, n*, and *t* represent the vehicle type, fuel type (gasoline or diesel), and year respectively; In this study, the main types of fuels consumed by on-road vehicles are gasoline and diesel. FN is the fleet number, which consists of public (bus and taxi) and private vehicles (passenger car, truck, and motorcycle). And the passenger car and truck are further divided into light, medium and heavy-duty classes; VKT represents the average kilometers vehicle traveled; FE is the fuel economy of vehicles (in liters per kilometer, *l*/km); *D* is the density of fuel type (in kg/*l*), which is 0.732 for gasoline and 0.875 for diesel; CR_n is the carbon ratio of fuel type, which is 85.5% for gasoline and 87% for diesel; 44/12 is the molecular weight ratio of carbon dioxide to carbon.

Table 2
NCV and EF for different fuel types.

Fuel type	NCV (MWh/t)	EF (tCO2/MWh)
Liquefied petroleum gas	13.1	0.227
Diesel	11.9	0.267
Gasoline	12.3	0.249
Kerosene	12.2	0.259
Fuel oil	11.2	0.279
Raw coal	5.8[a]	0.346[a]
Clean coal	7.2[a]	0.341[a]
Coking coal	7.8	0.341
Coal gas	11.9	0.267
Coke oven gas	10.8	0.160
Natural gas	13.3	0.202
Liquefied natural Gas	13.3	0.231
Electricity	/	0.739[b]
Heat	/	0.11(tCO2/GJ)[a]

Note.
[a] is from NDRC (2011).
[b] is the average value of Eastern China power grid released by NDRC (2009); others are from IPCC (2006).

Due to the lack of statistics on the fleet number further divided by fuel type, we make the following assumptions to enable the estimation, 1) all the buses and heavy-duty trucks use diesel; 2) all the motorcycles, taxis and light-duty passenger vehicles consume gasoline. For the rest of the vehicle classes, the proportions of vehicle either using gasoline or diesel are estimated by following the literature (Yan and Crookes, 2009; Han and Hayashi, 2008; Liu et al., 2013). The detailed data are listed in Table 3.

For the absence of officially published statistics on VKT and FE, they are complied from literature, and interpolated based on historical trends for those years lack of data. The details are listed in Table 4 and Table 5.

Though the SEAP method employed in this paper is compatible with the IPCC guidelines and is applicable to Chinese cities that have limited and fragmented energy data, the results may be different from those generated with the IPCC guidelines, since the former relies partially on city activities (for example, using fleet number as a proxy to estimate emissions from the transport sector), whereas the latter mainly depends on detailed energy consumption statistics. Moreover, even using the same SEAP method, the parameter settings in different literature may also cause diverse results. To quantify the uncertainties in CO_2 accounting, a Monte Carlo simulation approach was employed. This approach divides the uncertainties into two sources: activity levels (ALs) and emission factors (EFs). The ALs and EFs, which were assigned with a normal distribution and corresponding Coefficients of Variation (CVs, the ratio of the standard deviation to the average), were fed into the Monte Carlo simulations. For the ALs, the normal distributions with CVs of 10%, 20%, 20% and 16% were recommended for industrial,

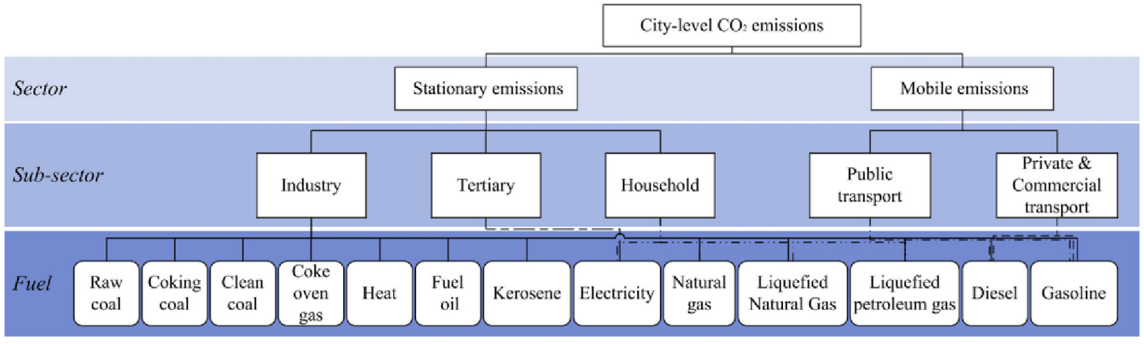

Fig. 2. SEAP framework for city-level CO_2 accounting.

Table 3
Proportion of vehicles using gasoline or diesel (%).

Vehicle type	Passenger vehicles				Trucks			
	Medium		Heavy		Light		Medium	
Fuel type	G	D	G	D	G	D	G	D
2003	72	28	17	83	12	88	10	90
2004	72	28	13	87	12	89	9	91
2005	73	27	12	88	10	90	8	92
2006	73	27	11	89	9	91	8	93
2007	73	27	10	90	8	92	7	93
2008	73	27	9	91	7	93	6	94
2009	74	26	8	92	6	94	6	94
2010	74	26	7	93	5	95	6	95
2011	74	26	6	94	4	96	5	95
2012	75	25	5	95	3	97	5	96
2013	75	25	4	96	2	98	4	96

Note: D and G means diesel and gasoline.

commercial, household and transport sectors (Zhao et al., 2012). The CVs for the EFs are also derived from Zhao et al.'s (2012) work according to a range of 95% confidence intervals. The CVs for different sectors are listed in Table S2 in the Supplementary Material. A total of 1000 trials were performed to estimate the uncertainties in CO_2 emissions accounting.

3.1.2. NTL data correction and urban extent extraction

Since the NTL is monitored with separate satellites (DMSP satellites F10, F12, F14, F15, F16), and the DN values are incompatible for direct use, we first removed the background noises and lights from the gas flares based on a method from Elvidge et al. (2009), then calibrated the data by using the methods proposed by Liu et al. (2012). However, unlike the approach of Liu et al. (2012), who used a city located in northeastern China (Jixi city) as the reference region, we chose Taizhou city, a city in Zhejiang province in YRD, as the reference city to calibrate the NTL images. The reason for the detailed calibration process is described in "1. Calibration processes of DMSP/OLS data in YRD" in the Supplementary Material.

Because of the relatively coarse spatial resolution of the OLS sensor, the calibrated NTL data are still suffer from the saturation effect, where lights detected in the center of large cities are too bright and cannot be distinguished (Elvidge et al., 2007). Besides, the spatial extent of lighted areas is often larger than the developed areas (blooming effect) as the diffuse and scattered lights detected by OLS sensor (Small et al., 2005). The saturation and blooming effects may cause potential estimation errors, especially in city center and suburban areas (Zhang et al., 2013). Based on the assumption of that vegetation cover and human activities are inversely spatial correlated, an improved Vegetation Adjusted NTL Urban Index, which combines NTL with time-series NDVI and population density (Meng et al., 2017), was employed to reduce the saturation and blooming problems after the calibration of original NTL dataset.

On the basis of the correction of NTL data, the urban extent was extracted from a city boundary through a dynamic threshold method, which has been used in a number of studies (Liu et al., 2012; Zhou et al., 2014). Here, as shown in Fig. 3, urban is defined as a built-up area where land has been developed and constructed on a large scale, including basic municipal public facilities, and where most of socio-economic activities occur. Its boundary varies over time due to the urbanization process. In contrast, a city refers to a jurisdictional unit with a fixed administrative boundary. Urban populations are one of the most important driving forces of urban expansion (Sutton et al., 2001; Han et al., 2009); thus, to increase the efficiency of urban extent extraction, we divided the 11 cities into 4 groups based on their urban population size. They are the super megacity, mega city, large city, and medium city, following a standard division used by the State Council of China (2014). Then, we determined an optimal threshold of NTL's DN value for each city group to separate urban and non-urban extents using urban built-up areas classified from Landsat ETM + images in 2000, 2005 and 2010 as references. Thresholds from 2000 were applied to the close years 2003–2004, values from 2005 were applied to 2005–2008, and thresholds from 2010 were applied to 2009–2013 (Table 6). With the support of the Landsat data, the accuracy could be much improved, and those pixels dominated by water and vegetation could be excluded from the urban extent.

However, the variation in the threshold value will definitely influence the final result. To quantify the uncertainties of urban extent extraction based on dynamic threshold method on the result of urban CO_2 emissions, we conducted a sensitivity analysis by measuring of the impact of threshold variation (1%, 5% and 10% increase or decrease) on urban CO_2 emissions while keeping other parameters constant.

3.2. Urban CO_2 emission modeling

3.2.1. Models for capturing the correlation between accounted CO_2 and NTL

Previous studies suggested the relationship between NTL and socio-environmental factors (such as population, GDP, and CO_2 emissions) follows a power-law relationship, where a relative change in one quantity results in a proportional relative change in the other quantity

Table 4
VKT by vehicle type in YRD cities (unit: 1000 km/vehicle/year).

Vehicle type	Bus	Taxi	Passenger vehicles			Trucks			Motorcycle
			Light	Medium	Heavy	Light	Medium	Heavy	
2003	58.0[a]	78.4[a]	21.2	40.7	40.7	25.4	52.9	52.9	9.0[c]
2004	58.8[a]	81.8[a]	21.4	41.1	41.1	25.7	53.5	53.5	9.0[c]
2005	59.7[a]	85.3[a]	21.8[b]	41.8[b]	41.8[b]	26.2[b]	54.5[b]	54.5[b]	8.0
2006	60.5[a]	88.7[a]	22.3 [b]	42.8 [b]	42.8[b]	26.8[b]	55.7[b]	55.7[b]	8.0
2007	61.4[a]	92.1[a]	22.9 [b]	44.1[b]	44.1[b]	27.5[b]	57.4[b]	57.4[b]	8.0
2008	62.2[a]	95.5[a]	23.7 [b]	45.6[b]	45.6[b]	28.5[b]	59.3[b]	59.3[b]	8.0
2009	63.0[a]	98.9[a]	24.6	47.3[b]	47.3[b]	29.6[b]	61.6[b]	61.6[b]	8.0
2010	63.9	102.3	25.7	49.3	49.3	30.8	64.2	64.2	7.0
2011	64.7	105.7	26.9	51.6	51.6	32.2	67.2	67.2	7.0
2012	65.5	109.0	28.2	54.2	54.2	33.8	70.5	70.5	7.0
2013	66.4	112.4	29.7	57.0	57.0	35.6	74.1	74.1	7.0

Note.
[a] is from Zhang et al. (2012).
[b] is from Liu et al. (2013).
[c] is from He et al. (2005). Others are interpolated.

Table 5
FE by vehicle type in YRD cities from 2003 to 2013 (*l*/100 km).

Vehicle type	Bus	Taxi	Passenger vehicles			Trucks				Motor
			Light	Medium	Heavy	Light		Medium	Heavy	
Fuel type	D	G	G	G	D	G	D	G	D	G
2003	33.3[a]	12.5[a]	10.2	37.3	24.2	12.6	15.0	33.4	27.4	2.7[a]
2004	33.3[a]	12.5[a]	10.0	37.3	23.8	12.5	14.8	33.4	26.9	2.7[a]
2005	33.3[a]	12.5[a]	9.8[b]	37.3[b]	23.4[b]	12.3[b]	14.6[b]	33.4[b]	26.5[b]	2.7[a]
2006	33.3[a]	12.5[a]	9.6	37.3	23.0	12.0	14.3	33.4	26.0	2.7[a]
2007	33.3[a]	12.5[a]	9.3	37.3	22.6	11.8	14.1	33.4	25.6	2.7[a]
2008	33.3[a]	12.5[a]	9.1[b]	37.3[b]	22.1[b]	11.6[b]	13.8[b]	33.4[b]	25.1[b]	2.7[a]
2009	33.3	12.5	8.8	37.3	21.7	11.3	13.5	33.4	24.5	2.7
2010	33.3	12.5	8.5	37.3	21.2	11.0	13.1	33.4	24.0	2.7
2011	33.3	12.5	8.2	37.3	20.7	10.7	12.8	33.4	23.5	2.7
2012	33.3	12.5	7.8	37.3	20.2	10.4	12.4	33.4	22.9	2.7
2013	33.3	12.5	7.5	37.3	19.7	10.1	12.0	33.4	22.3	2.7

Note.
[a] is from Zhang et al. (2012).
[b] is from Liu et al. (2013); Others are interpolated; D and G represents diesel and gasoline, respectively.

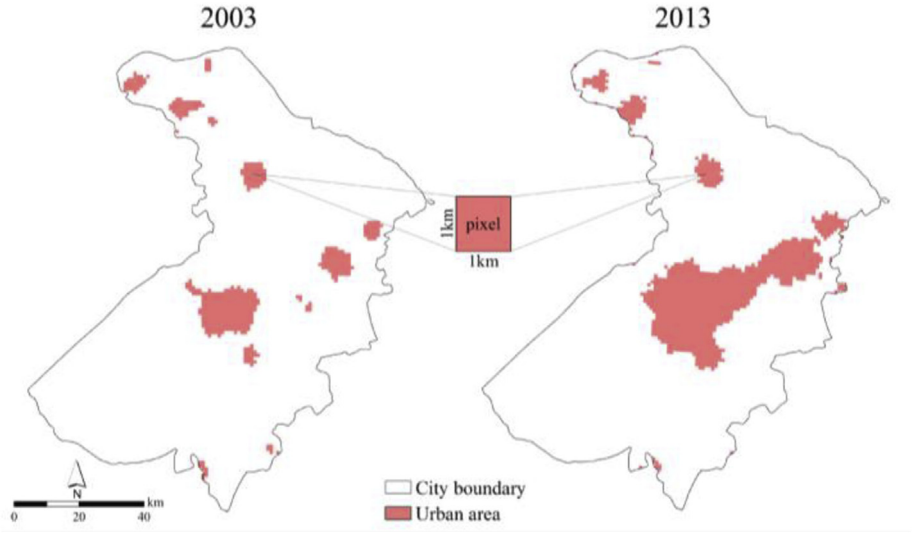

Fig. 3. Conceptual map of urban and city boundaries.

Table 6
Dynamic thresholds of four city groups for urban extent extraction.

City group	Cities included	Optimal threshold		
		2000	2005	2010
Super megacity (Urban Pop > 10million)	Shanghai	47	48	50
Mega city (5million < Urban Pop < 10million)	Nanjing, Suzhou	35	45	48
Large city (1million < Urban Pop < 5million)	Hangzhou, Changzhou, Wuxi, Zhenjiang, Nantong, Jinhua	31	35	46
Medium city (0.5million < Urban Pop < 1million)	Quzhou, Huzhou	25	30	38

(Sutton and Costanza, 2002).

To determine an improved method that can accurately and reliably capture the relationship between accounted CO_2 emissions and NTL, we developed the following three econometric models for comparison. Model 1 is based on pool-data regression and considers no spatiotemporal heterogeneities across cities and over time, which was also applied by Su et al. (2014). A double logarithm, as illustrated in Eq. (3), enabled comparison between the explanatory and explained variables and ascertained the elasticity of the DN on carbon emissions. Values of α and β represent the intercept and slope coefficient, ε is the error term.

$$\text{Model 1:}\quad \ln\left(\mathrm{AE}_{city_{i,t}}\right) = \alpha + \beta \times \ln\left(\mathrm{DN}_{\mathrm{city}_{i,t}}\right) + \varepsilon_{i,t} \tag{3}$$

To capture the influences of spatiotemporal heterogeneity among the 11 sample cities between 2003 and 2013, panel-data regression models were proposed. The subscripts i and t denote each city and year, respectively. Model 2 incorporates a city-specific coefficient (μ) in addition to DN, which was also used in studies by Meng et al. (2014) and Shi et al. (2016). Model 3 includes both the city-specific coefficient (μ) and time variable (σ) as additional explanatory variables. The values of i and t represent the specific city and year.

$$\text{Model 2:}\quad \ln\left(\mathrm{AE}_{city_{i,t}}\right) = \alpha + \beta \times \ln\left(\mathrm{DN}_{\mathrm{city}_{i,t}}\right) + \mu_i + \varepsilon_{i,t} \tag{4}$$

$$\text{Model 3:}\quad \ln\left(\mathrm{AE}_{city_{i,t}}\right) = \alpha + \beta \times \ln\left(\mathrm{DN}_{\mathrm{city}_{i,t}}\right) + \sigma_t + \mu_i + \varepsilon_{i,t} \tag{5}$$

3.2.2. Internal model validation

Using all the data for 11 cities covering 11 years (121 sample set in total), we performed an internal validation of Model 3 based on the following 2-fold cross-validation processes, and compared the result with that of Model 1 and 2 using the same data and validation process. i) All the data were randomly divided to two groups; ii) Data in each group were used in turn as training set for correlation analysis, while the remaining group was removed. Based on the coefficients derived from the regression models, the emissions for the remaining group were predicted; iii) The data in the removed group were used as references to calculate the difference between the predicted and observed values for each sample set; iv) The mean squares of the differences for all the sample set were calculated; v) By repeating the processes 1000 times through the Monte Carlo simulation, the model accuracy could be assessed through the median of root mean squared error. The lower the median is the more accurate the model will be.

3.2.3. Urban CO_2 emissions estimation

Based on the correlation between city-level accounted CO_2 emissions and DN that were deduced from either Eqs. (3) and (4), or (5), the pixel-level CO_2 emissions could be modeled using DN as a predictor. As differences exist between the accounted and modeled emissions, we used their ratio to further calibrate the CO_2 emissions at a pixel level, which is shown in Eq. (6).

$$CE_{urban_{i,t}} = \sum_k CE_{urban_{i,t}^k} = \sum_k \left(\frac{AE_{city_{i,t}}}{ME_{city_{i,t}}} \cdot ME_{urban_{i,t}^k} \right) \quad (6)$$

where $CE_{urban_{i,t}}$ is the calibrated urban CO_2 emissions in city i for year t. The value for k is the pixel within the urban area. AE_{city} represents the accounted city-level CO_2 emissions. ME_{city} and ME_{urban} are the modeled CO_2 emissions at a city and urban level.

4. Results

4.1. Model predictive power

Fig. 4 presents the correlation between NTL and the accounted CO_2 emissions that were estimated by the three models, and compares each model's predictive power that is measured by R^2. In model 1, the R^2 in both the sectoral and aggregated results was relatively high ($R^2 > 0.65$), which indicates that a significant correlation between the accounted CO_2 emissions and NTL, and at least 65% of the change in CO_2 emissions, could be explained by NTL. Meanwhile, the scattered points deviated from the fitting curve, as also suggested the existence of regional diversity among the cities. To eliminate the influence of spatial diversity on the carbon-NTL relationship, panel data analysis considering the city-specific effect as explained in Model 2 was conducted. It was found that the R^2 in Model 2 was significantly enhanced, with values over 0.97.

The results in Model 3 justify the importance of the incorporation of both space and time differences as explanatory variables in estimation. The R^2 values in Model 3 are all improved over those in models 1 and 2. In the estimation of the relationship between the city's total CO_2 emissions and corresponding NTL, the R^2 in Model 3 demonstrated the highest value, reaching 0.990. The city-specific coefficient (μ) for each city, as estimated by both Model 2 and 3, are listed in Table S5 in the Supplementary Material. However, for the time dummy variable (σ) in Model 3, a strong linear correlation with the year difference for mobile emissions was found, along with an inverted U-shape curve for stationary and total emissions (Fig. S5 in the Supplementary Material). All of the R^2 of the fitting lines were fairly high, which indicates a strong predictive power when using the fitting functions to estimate the time dummy variable σ.

In addition, when looking at the correlations between NTL and the accounted CO_2 emissions from the secondary industrial, tertiary industrial, and household sectors (as shown in Fig. S6 in the Supplementary Material), Model 3 still performed better than others as its minimum value of R^2 was 0.978. In sum, Model 3, which considers both the space and time differences across cities and over time, was proven to have a better predictive power than the other two models in modeling CO_2 emissions using NTL as a predictor.

4.2. Model validation

Fig. 5 shows the results of internal validation for three models using the same data set covering 11 cities from 2003 to 2013. It is found that the median of root mean square error (RMSE) for 1000 times of two-fold cross-validations was 0.438, 0.401 and 0.409 for stationary, mobile and total emissions respectively in Model 3, which was much lower than that in Model 1 and 2. It suggests that Model 3, which considers both the space and time differences, is more accurate.

Fig. 6 shows the external validation of our improved model's results at city level. Through the comparison of our accounted city-level CO_2 emissions (with 95% confidence intervals) in some specific cities with previous studies, it can be clearly found that the results of the same city can have much difference in different studies. For example, our estimates are all smaller than those from Wang et al. (2013), as they accounted the carbon emissions from industrial processes while we didn't. And our results are all larger than those from Yu et al. (2012), as we consider the emissions from heating while they ignored. But anyway, the changing trend and scale of all the results are similar with each other, which suggests the validity of our estimation.

Fig. 7 shows the external validation of our results at pixel level by comparing our modeled 1 km-pixel CO_2 emissions with those estimated by Oda and Maksyutov (2011) (available at http://odiac.org/dataset.html) in YRD in 2010. It is found that there was an extremely high emission point in Oda and Maksyutov's estimation (the blue peak in Fig. 7d) while not in ours. It is because in addition to downscaling the national fossil fuel-induced CO_2 emissions to 1 km pixel level using NTL as a proxy, Oda and Maksyutov (2011) also separately estimated emissions from point sources using a global power plant database. Except the difference in point source emission, it is clear that our result can better describe the spatial distribution and heterogeneity of urban CO_2 emissions as the fluctuation of our estimates along the line transact was more significant (the red curve in Fig. 7d) than Oda and Maksyutov's, and the spatial pattern of our modeled urban CO_2 emissions (Fig. 7c) was closer to the distribution of urban extent (Fig. 7a).

4.3. Urban CO_2 emissions in YRD

Based on the results from Model 3, Fig. 8 illustrated the dynamic change in the calibrated CO_2 emissions from urban and non-urban areas in the YRD cities. As shown in Fig. 8a, urban CO_2 emissions increased four-fold, from 194 million tons in 2003 to 714 million tons in 2013, with its share in total emissions continuously increasing from 37% to 57%. When looking at per capita CO_2 emissions (Fig. 8b), although they increased at a similar rate of 10% per annum in urban and non-urban areas, urban areas had a lower value, with an increase from 6 to 15 tons/capita. Furthermore, we also probed into the change in carbon density. As shown in Fig. 8b, the carbon density of urban land ascended sharply from 17000 tons/km^2 in 2003–27000 tons/km^2 in 2007, and then fluctuated around 28000 tons/km^2 thereafter, which is 3–4 times larger than that of non-urban lands. The faster growth in urban CO_2 emissions (22%/yr) compared to that in urban expansion (9%/yr) from 2003 to 2007 is the main reason for the quick increase in carbon density in urban areas. However, after 2007, the increase in urban CO_2 emissions slowed at an annual rate of 9% and resulted in the stabilization of carbon density.

Second, we also investigated the spatiotemporal patterns of urban CO_2 emissions and illustrated the medium value of Monte Carlo simulation in Fig. 9. Generally, the urban CO_2 emissions demonstrated a

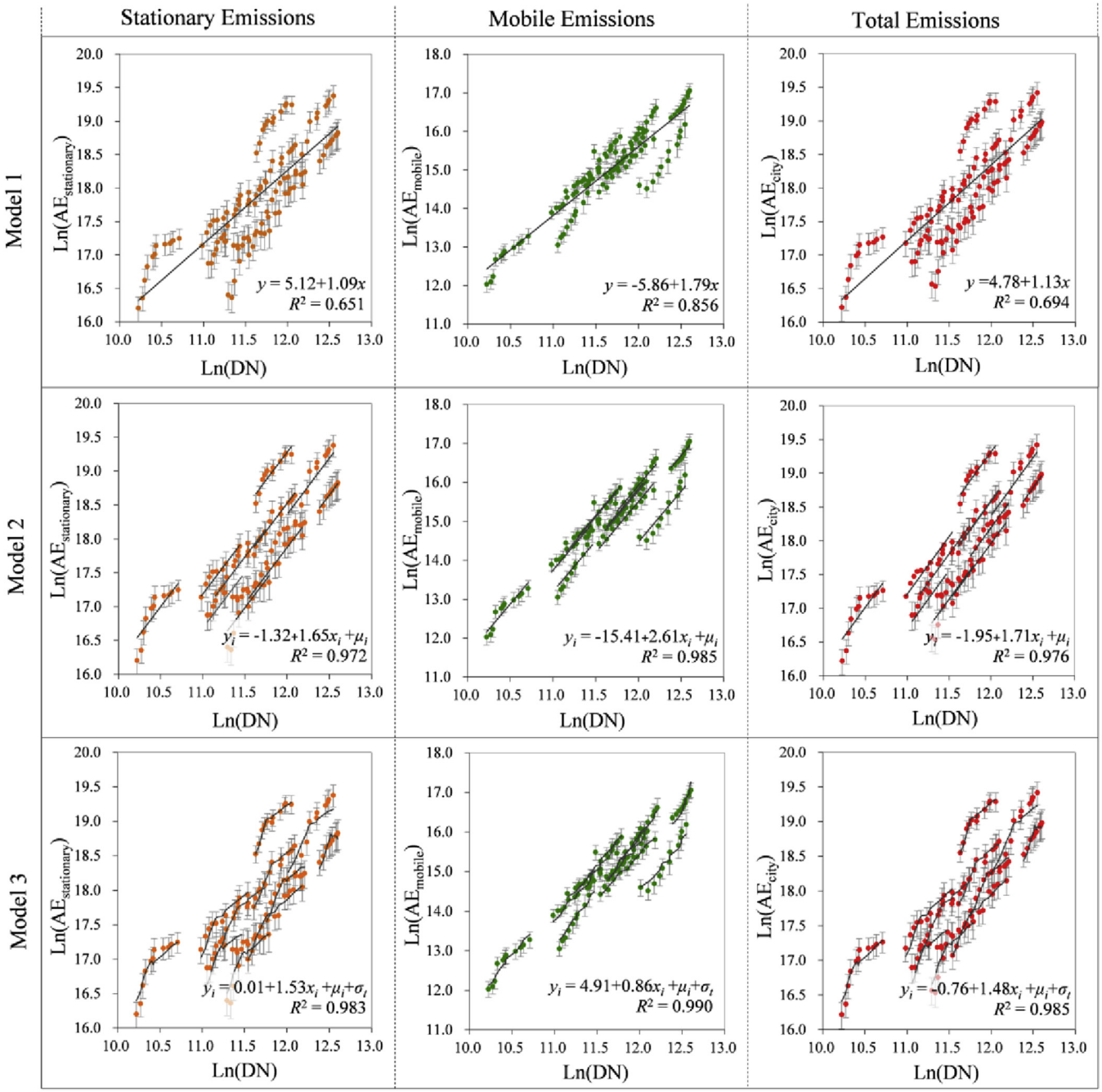

Fig. 4. Comparison of model predictive power. Relationship between city-level NTL and the accounted CO_2 emissions from stationary sources (left), mobile sources (middle), and for the total city (right) in 2003–2013. Scattered points represent the median value of the Monte Carlo simulation results. The error bars represent the upper and lower bound of 95% confidence intervals.

significant increase and expansion over the whole YRD region. However, the spatial distribution of the increase was not even. High emissions were found in the northern and northwestern parts of the YRD, such as in Suzhou and Nanjing. In contrast, cities in eastern YRD had a relatively low urban carbon density (Fig. 9a). To observe the dynamic changes and spatial differences of urban carbon emissions clearly, we calculated the annual growth rate of carbon density in each 1 km × 1 km pixel from 2003 to 2013, and classified the change into five grades according to the natural breaking methods (Brewer and Pickle, 2002). As shown in Fig. 9b, two types of significant growth were detected. One was the newly built growth in the outer suburbs of each city, where it was non-urban in 2003 but became urban in 2013. Another is the rapid growth in the peri-urban areas adjacent to the urban centers. Notably, the growth in the cities close to Shanghai, such as Suzhou, Nantong, and Wuxi, were particularly sharp. Moreover, the change in urban CO_2 emissions per capita was also classified into five grades using the same breaking method (Fig. 9c). Between 2003 and 2013, the fastest growth occurred in Suzhou, whose urban population was approximately 7.7 million and the population density was 770 cap/km^2 in 2013, but the per capita carbon increased 4-fold, from 10.7 to 41.4 ton/cap. In contrast, Shanghai had an urban population of over 13 million and 3800 cap/km^2 of population density. However, its per capita urban carbon demonstrates the slowest growth from 8.3 to 12.3 ton/cap. This suggests that, on a per capita basis, large and compact

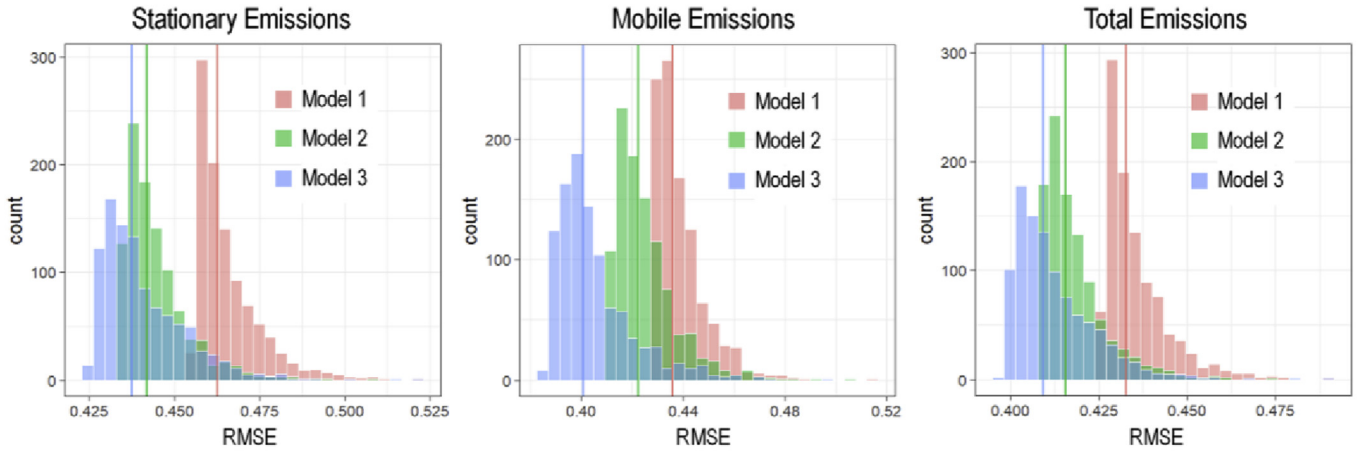

Median of RMSE for 1000 times of two-fold cross-validations	Model 1	Model 2	Model 3
Stationary emissions	0.463	0.442	0.438
Mobile emissions	0.436	0.422	0.401
Total emissions	0.433	0.416	0.409

Fig. 5. Internal validation of model results. The vertical lines are the median of RMSE for 1000 times of two-fold cross-validations.

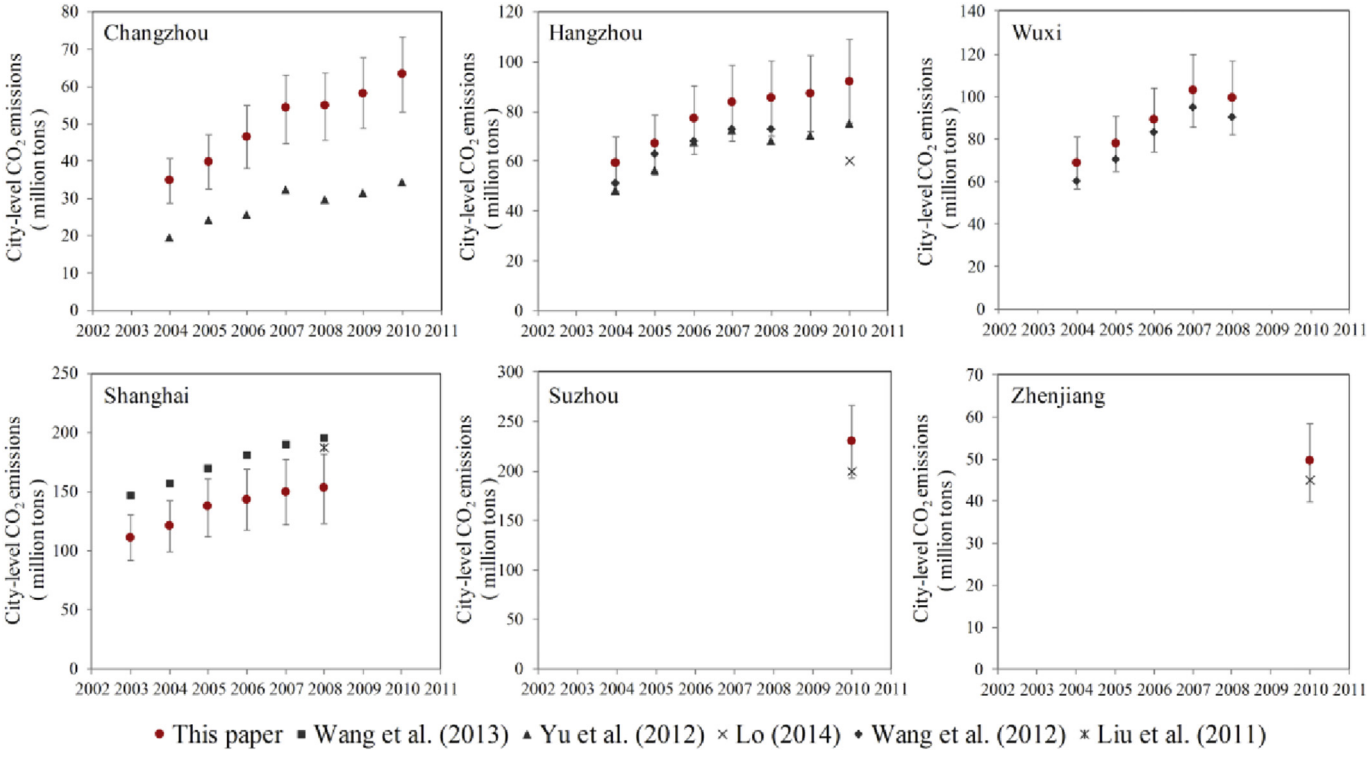

Fig. 6. City-level external validation of our method (Liu et al., 2011; Lo, 2014; Wang et al., 2012).

cities are usually more carbon efficient than small and sprawling cities (World Bank, 2010).

5. Discussions

5.1. Uncertainties and limitations of our method

The urban CO_2 emissions were calculated from the summation of gridded emissions within the urban extent. Since we assumed that relationship between 1 km grid level CO_2 emissions and NTL was consistent with that at city-level, thus the uncertainty of each gridded emissions value should be the same as that of the accounted city-level emissions. Therefore, the uncertainties in urban CO_2 emissions modeling should derive from the following two approaches.

First, city-level CO_2 emissions were accounted by the SEAP approach. Based on a Monte Carlo simulation, the mean uncertainties

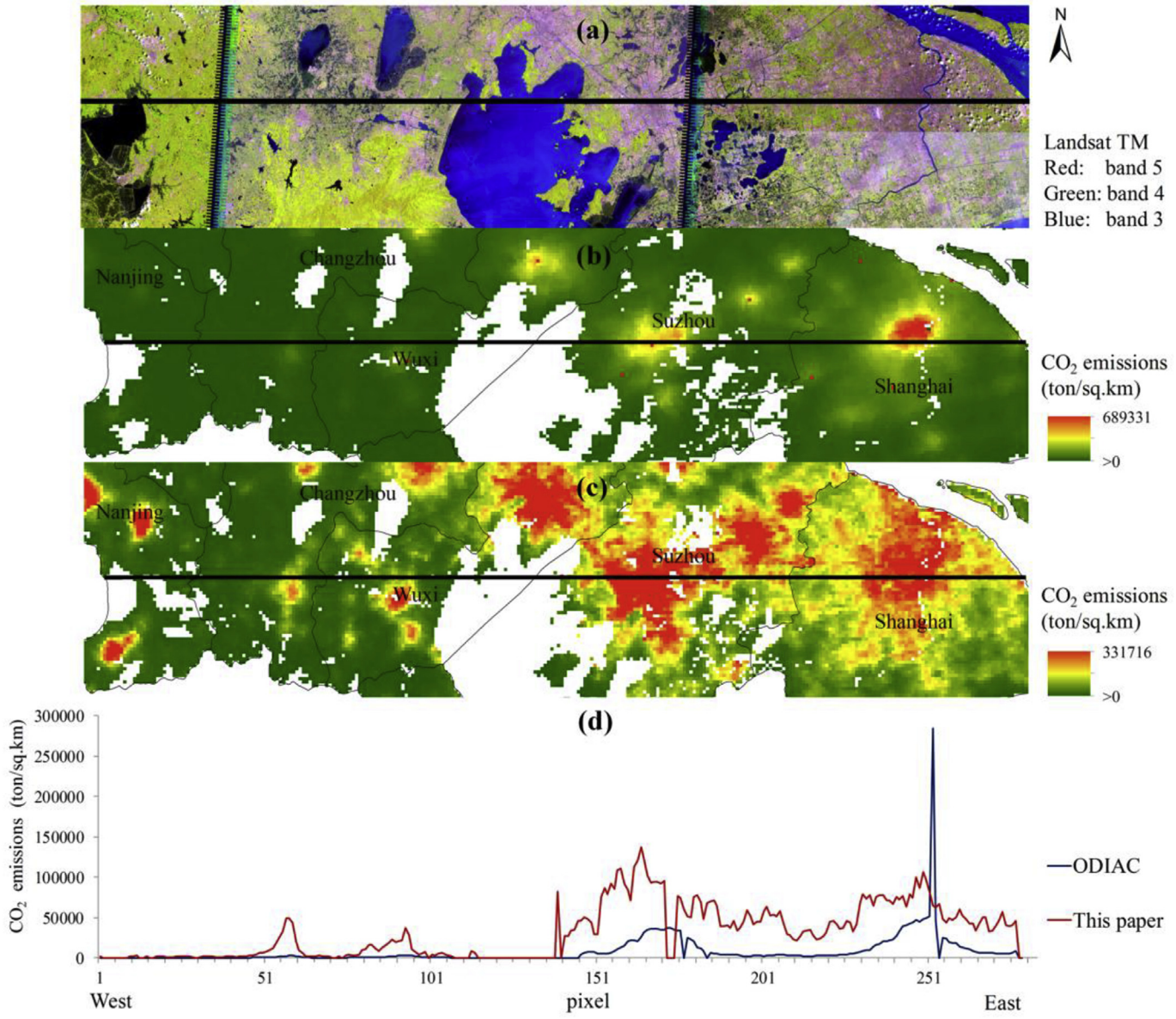

Fig. 7. Pixel-level external validation of our results. a) Landsat image in 2010; b) Pixel-level CO_2 emissions in 2010 estimated by Oda and Maksyutov (2011); c) Pixel-level CO_2 emissions in 2010 estimated by our method; d) Value comparison in a line transect of YRD in 2010.

(with 95% confidence intervals) of our accounted CO_2 emissions from a stationary source, mobile source, and city total, for the 11 cities between 2003 and 2013, were −17.5% to 18.0%, −18.0%–19.7%, and −17.5% to 18.0%, respectively. As a comparison to other studies, the uncertainty in China's CO_2 estimation conducted by Gregg et al. (2008) ranged from 15 to 20%.

Second, the urban extent was extracted by a dynamic threshold approach. By comparing our estimated urban extent in some of the selected cities for each city group in 2005, 2010, and 2013 with the land use and cover data classified from Landsat images that were obtained from the Data Center for Resources and Environmental Sciences, at the Chinese Academy of Sciences (http://www.resdc.cn) and the Global Institute for Urban and Regional Sustainability (http://www.giurs.com/), the reliability of the dynamics of urban extent could be measured by Kappa and Overall Accuracy (OA) indices, which are two widely used coefficients to assess the classification accuracy of remote sensing images (Cohen, 1960; Fitzgerald and Lees, 1994). As illustrated in Fig. S7 - Fig. S9 in the Supplementary Material, the average Kappa and OA were 0.37 and 89.17% in 2005, 0.38 and 88.41% in 2010, and 0.38 and 84.53% in 2013, suggesting that the dynamic threshold method can capture the change in urban extent with a relatively high accuracy.

Fig. 10 shows how every 1%, 5% and 10% increase or decrease of the DN threshold will affect the final urban CO_2 emissions. We found that the sensitivity of the urban CO_2 emissions to DN threshold differed from years and increased when the variation in threshold became larger. Specifically, every 1% change in the DN threshold would contribute to −4.1–2.5% changes in urban CO_2 emissions. A 5% threshold variation would cause −7.9–9.7% changes in emissions. When the threshold variation increased to 10%, the urban CO_2 emissions would change by 15.8–20.1%, which was as large as the mean uncertainties in the city-level CO_2 accounting. This suggests that urban extent extraction was as important as city-level CO_2 accounting for reducing the uncertainties of urban CO_2 modeling. In the future, more emphasis should be put on improving the quality of statistical energy data, raising the accuracy of carbon emissions factors in study area and improving the reliability of the extracted urban extent.

Some limitations still remain and require further research. First,

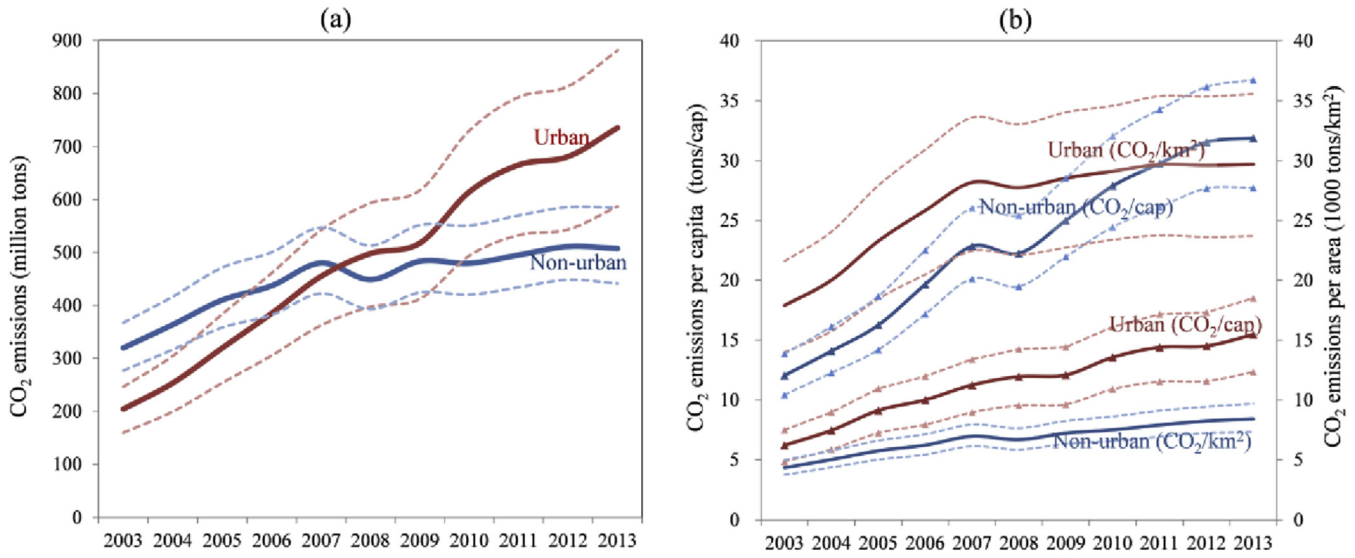

Fig. 8. Urban and non-urban CO_2 emissions in YRD cities 2003–2013. (a) Amount of emissions; (b) emissions per capita and per area. The solid lines represent the median value of the Monte Carlo simulation results. The broken lines represent the upper and lower bounds of the 95% confidence intervals.

only three years of Landsat images were used as a reference in the urban extent extraction, which limits the reliability of the results. Second, the significant correlation between city-level CO_2 emissions per sector and NTL (as shown in Fig. 4 and Fig. S6 in the Supplementary Material) is only from the perspective of statistical analysis, it may not mean there is real correlation between pixel-level NTL and CO_2 emissions per sector. Without the detailed information about the land type of and the human activity upon the pixel, our method can only represent mixed CO_2 emissions from different sectors at pixel level. Third, the external model validation at pixel level is the comparison of our results with other researcher's model results rather than the comparison with the real ground-based CO_2 emission monitoring data. In the future, possible improvements could include the following aspects. a) Collecting more Landsat images to raise the accuracy of urban extent extraction; b) Combining more detailed land use and human activity data (for example, high-resolution land use and cover maps, and point-of-interest data of infrastructure distribution) to obtain more information about urban pixel so that pixel-level CO_2 emissions per sector could be estimated; c) Conducting a true external validation by running an atmospheric transport-dispersion model based on our modeled 1 km pixel-level CO_2 emission data, and comparing results with ground-based CO_2 monitoring data (for example, the TANSAT carbon satellite data, which has a 1 × 2 km spatial resolution and was released in 2017 (http://satellite.nsmc.org.cn/PortalSite/Data/Satellite.aspx)).

5.2. Potential uses

Based on the proposed method for estimating urban CO_2 emissions, several potential uses can be derived. They include but are not limited to the following.

The proposed method can serve as a decision-support tool for updating and investigating the dynamic changes in urban CO_2 emissions at a relatively high spatial resolution. They can also be used as input for carbon-cycle and climate-simulation models.

The exploration of urban CO_2 emissions and their variation provides insights for follow-up analysis. Combined with the spatial data of socioeconomic variables (e.g., GDP, population), infrastructure distribution, and land use/cover, the socioeconomic and biophysical factors that drive urban CO_2 change could also be quantified.

Data availability and quality are recognized as the major obstacles for accurately estimating the spatial and temporal patterns of CO_2 emissions. The pixel-level CO_2 estimation by downscaling from city-level CO_2 inventory rather than from nation and sub-national regions, as shown in our case study, provides a possibility to address this gap. Though it requires not only the statistical energy data but also the activity data (for example, vehicle fleet number), we believe it is feasible to collect similar data for other Chinese cities as well. Similar database for cities in other countries should also be explored via international collaboration.

6. Conclusions

In this study, we propose an improved method for quantifying urban CO_2 emissions using NTL as a proxy. In contrast to previous research, we bring forward the existing CO_2 inventories from national and provincial levels to city level, correct the saturation problem of NTL, and considers the spatiotemporal heterogeneities across cities and over time in modeling the NTL-CO_2 correlation. Although the correlation parameters derived in the YRD were city specific and cannot be directly used for other cities/regions in China, the developed method can be applied to other areas, even if they do not have a detailed energy balance table; furthermore, our method is proven to better capture the correlations between NTL and CO_2 emissions from different sectors (that is industrial, tertiary, household, and transport sectors) or for city aggregates compared to the methods reported in previous studies. Our method is a supplement to existing approaches for modeling urban CO_2 emissions. Moreover, it helps understand the spatiotemporal dynamics and causal factors of urban carbon emissions. The major findings are as follows.

First, through the internal and external validations, our proposed method was proven to have better performance for capturing the NTL-CO_2 correlation compared to the methods employed in previous studies (Su et al., 2014; Meng et al., 2014; Shi et al., 2016), and for describing the spatial distribution and heterogeneity of CO_2 emissions. Second, between 2003 and 2013, the total CO_2 emissions in the YRD more than doubled, from 524 to 1243 million tons, during which time, the contribution from urban areas also increased significantly, from 37% to 57%. On a per capita basis, the mean CO_2 emissions in urban areas increased from 6 to 15 tons/cap in the last decade, and large cities are usually more carbon efficient than small and medium cities. Third, the urban carbon density increased sharply from 2003 to 2007 and became steady approximately 28000 tons/km^2 afterward. Spatially, urban

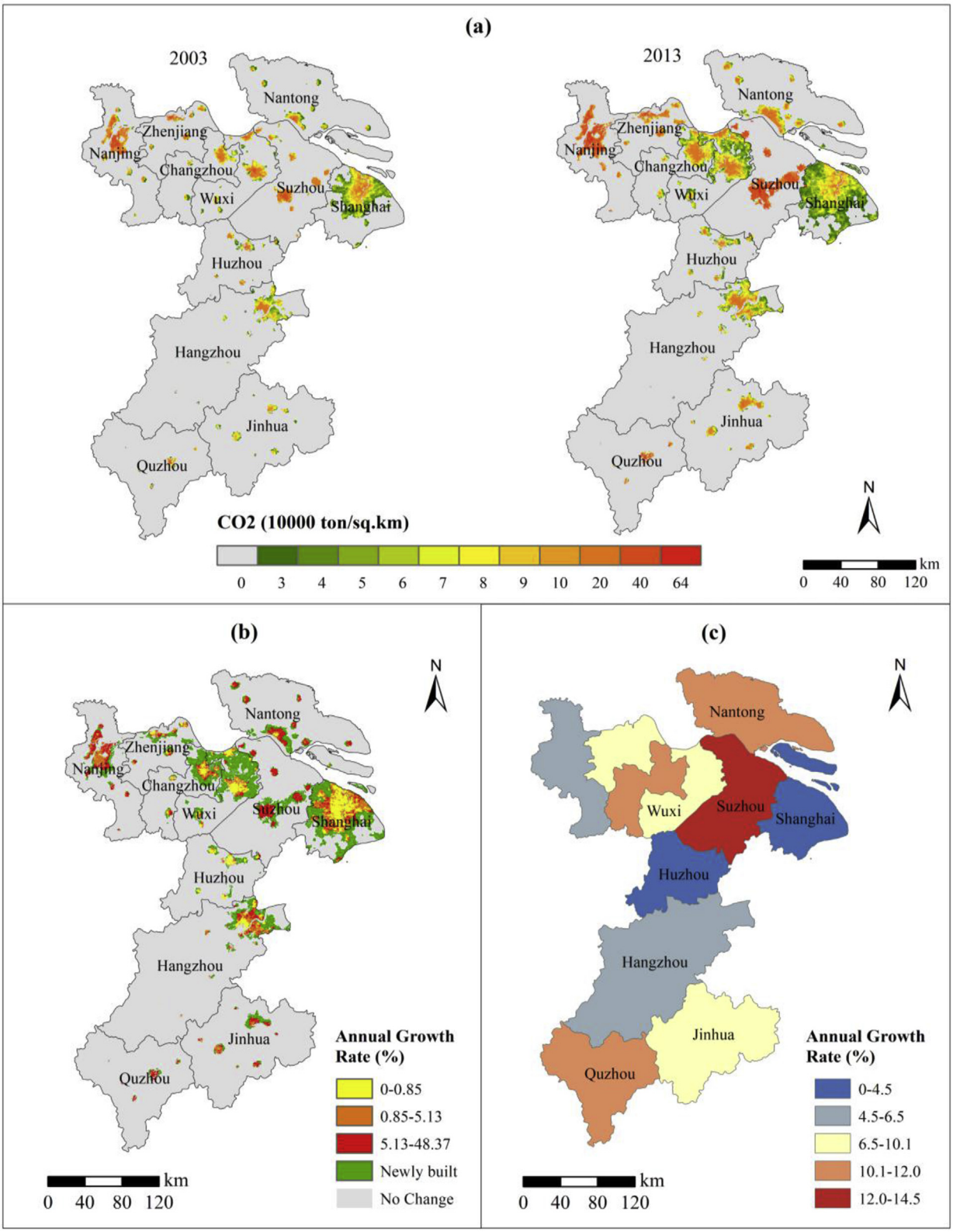

Fig. 9. Spatiotemporal variation of urban CO_2 emissions in the YRD based on the median value of a Monte Carlo simulation. (a) Spatial distribution of urban CO_2 in 2003 and 2013; (b) change in carbon density in 2003–2013; and (c) change in per capita urban CO_2 in 2003–2013.

sprawl in the outer suburbs, and the regional transfer of labor and resource intensive industries from the core cites to peri-urban areas in adjacent cities, led to rapid growth of urban carbon density in corresponding areas.

Acknowledgments

The work of Ji Han was supported by the National Key R&D Program of China [grant number 2017YFC0505703]; the National Natural Science Foundation of China [grant number 41401638];

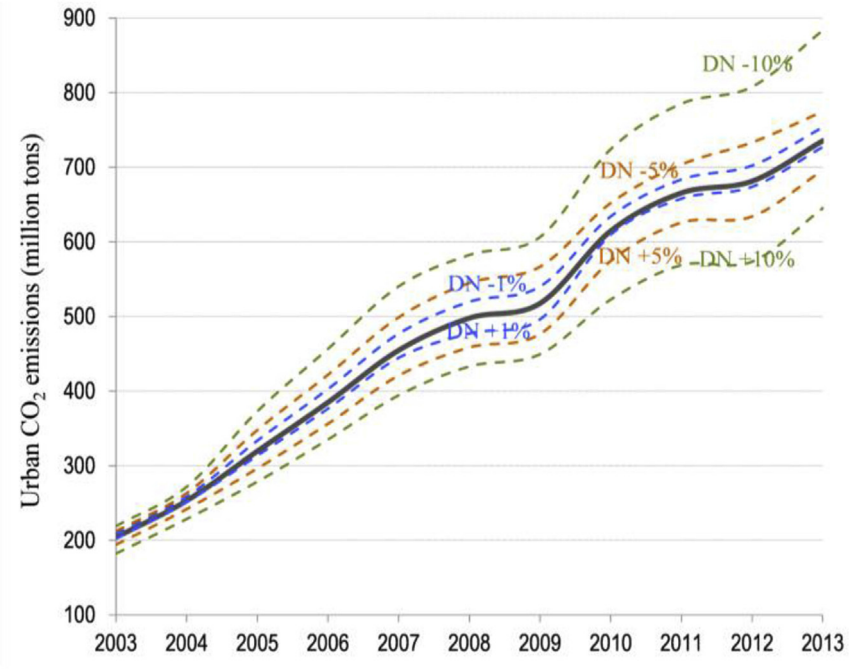

Fig. 10. Sensitivity of urban CO_2 emissions to DN threshold variation based on the median value of a Monte Carlo simulation.

Ministry of Education in China Project of Humanities and Social Sciences [grant number 14YJAZH028]; Shanghai Philosophy of Social Sciences Planning Project [grant number 2014BCK001]. Hanwei Liang acknowledges the funding from the Startup Foundation for Introducing Talent of NUIST [grant number 2243141501003-2015r003] and the Shanghai Key Lab for Urban Ecological Processes and Eco-Restoration of China [grant number SHUES2015A04]. Zhi Cao would thank National Key R&D Program of China [grant number 2016YFA0602802] for financial support. Liang Dong would appreciate the financial support from the project of "Smart Industrial Parks (SIPs) in China: towards Joint Design and Institutionalization" [grant number 467-14-003], as well as National Social Science Foundation [grant number 15ZDB163].

Appendix A. Supplementary data

Supplementary data related to this article can be found at http://dx.doi.org/10.1016/j.envsoft.2018.05.008.

References

Albert, H.B., Michael, F., Birgit, K., 2015. The spatial dimension of urban greenhouse gas emission: analyzing the influence of spatial structures and LULC patterns in European cities. Landsc. Ecol. 30, 1195–1205.

Asefi-Najafabady, S., Rayner, P.J., Gurney, K.R., Mcrobert, A., Song, Y., Coltin, K., Baugh, K., 2014. A multiyear, global gridded fossil fuel CO_2 emission data product: evaluation and analysis of results. J. Geophys. Res. 119, 10213–10231.

Bennett, M.M., Smith, L.C., 2017. Advances in using multitemporal night-time lights satellite imagery to detect, estimate, and monitor socioeconomic dynamics. Remote Sens. Environ. 192, 176–197.

Brewer, C.A., Pickle, L., 2002. Evaluation of methods for classifying epidemiological data on choropleth maps in series. Ann. Assoc. Am. Geogr. 92, 662–681.

Cai, H., Xie, S.D., 2007. Estimation of vehicular emission inventories in China from 1980 to 2005. Atmos. Environ. 41, 8963–8979.

Cao, X., Wang, J.M., Chen, J., Shi, F., 2014. Spatialization of electricity consumption of China using saturation-corrected DMSP-OLS data. Int. J. Appl. Earth Obs. Geoinf. 28, 193–200.

Carney, S., Green, N., Wood, R., Read, R., 2009. Greenhouse Gas Emissions Inventories for Eighteen European Regions, $EUCO_2$ 80/50 Project Stage 1: Inventory Formation. http://territorio.regione.emilia-romagna.it/programmazione-territoriale/governance/euco-80-50/greenhousegasemissionsinventories.pdf [accessed 18.05.21].

Chen, X., Nordhaus, W.D., 2011. Using luminosity data as a proxy for economic statistics. Proc. Natl. Acad. Sci. U.S.A. 108, 8589–8594.

Cohen, J., 1960. A coefficient of agreement for nominal scales. Educ. Psychol. Meas. 20 (1), 37–46.

CoM (The Covenant of Mayors), 2010. How to Develop a Sustainable Energy Action Plan-guidebook. [accessed 16.01.08]. http://www.eumayors.eu/IMG/pdf/seap_guidelines_en-2.pdf.

Edward, L.G., Matthew, E.K., 2010. The greenness of cities: carbon dioxide emissions and urban development. J. Urban Econ. 67, 404–418.

Elvidge, C.D., Cinzano, P., Pettit, D.R., Arvesen, J., Sutton, P.C., Small, C., et al., 2007. The Nightsat mission concept. Int. J. Rem. Sens. 28, 2645–2670.

Elvidge, C.D., Ziskin, D., Baugh, K.E., Tuttle, B.T., Ghosh, T., Pack, D.W., et al., 2009. A fifteen year record of global natural gas flaring derived from satellite data. Energies 2, 595–622.

Fitzgerald, R.W., Lees, B.G., 1994. Assessing the classification accuracy of multisource remote sensing data. Remote Sens. Environ. 47 (3), 362–368.

Gregg, J.S., Andres, R.J., Marland, G., 2008. China: emissions pattern of the world leader in CO_2 emissions from fossil fuel consumption and cement production. Geophys. Res. Lett. 35http://dx.doi.org/10.1029/2007GL032887. L08806.

Gurney, K.R., Romero-Lankao, P., Seto, K.C., Hutyra, L.R., Duren, R., Kennedy, C., et al., 2015. Track urban emissions on a human scale. Nature 525, 179–181.

Han, J., Hayashi, Y., 2008. Assessment of private car stock and its environmental impacts in China from 2000 to 2020. Transport. Res. Transport Environ. 13, 471–478.

Han, J., Hayashi, Y., Cao, X., Imura, H., 2009. Evaluating land use change in rapidly urbanizing China: a case study of Shanghai. J. Urban Plann. Dev. 135, 166–171.

He, K.B., Huo, H., Zhang, Q., He, D.Q., An, F., Wang, M., et al., 2005. Oil consumption and CO_2 emissions in China's road transport: current status, future trends, and policy implications. Energy Pol. 33, 1499–1507.

ICLEI (Local Governments for Sustainability), 2009. International Local Government Greenhouse Gas Emissions Analysis Protocol. [accessed 16.01.05]. http://archive.iclei.org/fileadmin/user_upload/documents/Global/Progams/CCP/Standards/IEAP_October2010_color.pdf.

IPCC (Intergovernmental Panel on Climate Change), 2006. 2006 IPCC Guidelines for National Greenhouse Gas Inventories. Institute for Global Environmental Strategies, Hayama.

Kennedy, C., Steinberger, J., Gasson, B., Hansen, Y., Hillman, T., Havranek, M., et al., 2009. Greenhouse gas emissions from global cities. Environ. Sci. Technol. 43, 7297–7302.

Kennedy, C., Steinberger, J., Gasson, B., Hansen, Y., Hillman, T., Havranek, M., et al., 2010. Methodology for inventorying greenhouse gas emissions from global cities. Energy Pol. 38, 4828–4837.

Liang, H.W., Tanikawa, H., Matsuno, Y., Dong, L., 2014. Modeling in-use steel stock in China's buildings and civil engineering infrastructure using time-series of DMSP/OLS nighttime lights. Rem. Sens. 6, 4780–4800.

Liu, Z., Geng, Y., Xue, B., 2011. Inventorying energy-related CO_2 for city: Shanghai study. Energy Procedia 5, 2303–2307.

Liu, Z.F., He, C.Y., Zhang, Q.F., Huang, Q.X., Yang, Y., 2012. Extracting the dynamics of urban expansion in China using DMSP-OLS nighttime light data from 1992 to 2008. Landsc. Urban Plann. 106, 62–72.

Liu, Y., Wang, Y., Huo, H., 2013. Temporal and spatial variations in on-road energy use and CO_2 emissions in China, 1978-2008. Energy Pol. 61, 544–550.

Lo, K., 2014. Energy-related carbon emissions of China's model environmental cities. Geogr. J. 2014, 1–7.

Ma, X.L., Tong, X.H., Liu, S.C., Luo, X., Xie, H., Li, C.M., 2017. Optimized sample selection in SVM classification by combining with DMSP-OLS, landsat NDVI and globeland 30 products for extracting urban built-up areas. Rem. Sens. 9 (3), 236.

Meng, L.N., Graus, W., Worrell, E., Huang, B., 2014. Estimating CO_2 (carbon dioxide) emissions at urban scales by DMSP/OLS (Defense Meteorological Satellite Program's Operational Linescan System) nighttime light imagery: methodological challenges and a case study for China. Energy 71, 468–478.

Meng, X., Han, J., Huang, C., 2017. An improved vegetation adjusted nighttime light urban index and its application in quantifying spatiotemporal dynamics of carbon emissions in China. Rem. Sens. 9, 829.

NBS (National Bureau of Statistics), 2015. China Statistical Yearbook. China Statistics Press, Beijing.

NDRC (National Development and Reform Commission), 2009. Baseline Emission Factors for Regional Power Grids in China. [accessed 16.01.15]. Chinese. http://qhs.ndrc.gov.cn/qjfzjz/200907/t20090703_289357.html.

NDRC (National Development and Reform Commission), 2011. Provincial Guidelines for Greenhouse Gas Inventories. [accessed 16.01.03]. Chinese. http://www.cbcsd.org.cn/sjk/nengyuan/standard/home/20140113/download/shengjiwenshiqiti.pdf.

Oda, T., Maksyutov, S., 2011. A very high-resolution (1 km x 1 km) global fossil fuel CO_2 emission inventory derived using a point source database and satellite observations of nighttime lights. Atmos. Chem. Phys. 11, 543–556.

Shi, K.F., Chen, Y., Yu, B.L., Xu, T.B., Chen, Z.Q., Liu, R., et al., 2016. Modeling spatiotemporal CO2 (carbon dioxide) emission dynamics in China from DMSP-OLS nighttime stable light data using panel data analysis. Appl. Energy 168, 523–533.

Small, C., Pozzi, F., Elvidge, C.D., 2005. Spatial analysis of global urban extent from DMSP-OLS night lights. Remote Sens. Environ. 96 (3), 277–291.

State Council of China, 2014. Notification on Adjusting the Standards for City Scale Division. [accessed 17.04.28]. http://www.gov.cn/.

Su, Y.X., Chen, X.Z., Li, Y., Liao, J.S., Ye, Y.Y., Zhang, H.G., et al., 2014. China's 19-year city-level carbon emissions of energy consumptions, driving forces and regionalized mitigation guidelines. Renew. Sustain. Energy Rev. 35, 231–243.

Sutton, P.C., Costanza, R., 2002. Global estimates of market and non-market values derived from nighttime satellite imagery, land cover, and ecosystem service valuation. Ecol. Econ. 41 (3), 509–527.

Sutton, P., Roberts, D., Elvidge, C., Baugh, K., 2001. Census from Heaven: an estimate of the global human population using night-time satellite imagery. Int. J. Rem. Sens. 22, 3061–3076.

Wang, H., Zhang, R., Liu, M., Bi, J., 2012. The carbon emissions of Chinese cities. Atmos. Chem. Phys. 12, 6197–6206.

Wang, Y.S., Ma, W.C., Tu, W., Zhao, Q., Yu, Q., 2013. A study on carbon emissions in Shanghai 2000-2008, China. Environ. Sci. Pol. 27, 151–161.

WBCSD and WRI (World Business Council for Sustainable Development and World Resources Institute), 2004. A Corporate Accounting and Reporting Standard. Conches, Washington, DC.

Whittaker, C., McManus, M.C., Smith, P., 2013. A comparison of carbon accounting tools for arable crops in the United Kingdom. Environ. Model. Software 46, 228–239.

World Bank, 2010. Cities and Climate Change: an Urgent Agenda. World Bank, Washington, DC.

Xie, Y., Weng, Q., 2017. Spatiotemporally enhancing time-series DMSP/OLS nighttime light imagery for assessing large-scale urban dynamics. ISPRS J. Photogrammetry Remote Sens. 128, 1–15.

Yamina, S., Isabella, M., Albana, K., Sandor, S., 2014. Guidebook How to Develop a Sustainable Energy Action Plan (SEAP) in South Mediterranean Cities. [accessed 16.01.08]. http://iet.jrc.ec.europa.eu/energyefficiency/system/tdf/guidebook_final_english.pdf?file=1&type=node&id=9031.

Yan, X., Crookes, R.J., 2009. Reduction potentials of energy demand and GHG emissions in China's road transport sector. Energy Pol. 37, 658–668.

Yu, W., Pagani, R., Huang, L., 2012. CO_2 emission inventories for Chinese cities in highly urbanized areas compared with European cities. Energy Pol. 47, 298–308.

Zhang, Q., Schaaf, C., Seto, K.C., 2013. The vegetation adjusted NTL urban index: a new approach to reduce saturation and increase variation in nighttime luminosity. Remote Sens. Environ. 129 (2), 32–41.

Zhang, Q., Tao, X., Yang, P., 2012. Research on carbon emissions from metropolis urban passenger transport and countermeasures. China Pop. Resour Environ. 22, 35–42.

Zhao, Y., Nielsen, C.P., McElroy, M.B., 2012. China's CO_2 emissions estimated from the bottom up: recent trends, spatial distributions, and quantification of uncertainties. Atmos. Environ. 59, 214–223.

Zhou, Y.Y., Smith, S.J., Elvidge, C.D., Zhao, K.G., Thomson, A., Imhoff, M., 2014. A cluster-based method to map urban area from DMSP/OLS nightlights. Remote Sens. Environ. 147, 173–185.